UMSHA Press

AJCMI
Avicenna Journal of Clinical Microbiology and Infection

Avicenna J Clin Microbiol Infect 2026;13(3): x-x. doi:10.34172/ajcmi.3777

http://ajcmi.umsha.ac.ir

Original Article

Screening of Key Auto-Induction Medium Components Affecting Recombinant Endolysin Production Against Antibiotic-Resistant *Acinetobacter baumannii* Using a Plackett–Burman Design

Dorna Rafighi[1], Mehrdad Azin[2*], Abbas Akhavan Sepahi[3], Nayyereh Alimadadi[1]

[1]Department of Biology, SR.C., Islamic Azad University, Tehran, Iran
[2]Department of Biotechnology, Iranian Research Organization for Science & Technology, Tehran, Iran
[3]Department of Microbiology, NT.C., Islamic Azad University, Tehran, Iran

Article history:
Received: September 7, 2025
Revised: October 26, 2025
Accepted: January 4, 2026
ePublished: Xx xx, 2026

***Corresponding author:**
Mehrdad Azin,
Email: azin@irost.ir

Abstract

Introduction: The global rise in antibiotic resistance has made infections caused by drug-resistant bacteria, such as *Acinetobacter baumannii*, a major public health concern. Consequently, the development of novel and efficient treatment strategies is urgently required. This study employed a Plackett–Burman design (PB) to identify the key autoinduction medium components affecting recombinant endolysin production in *Escherichia coli* BL21 (DE3) and its lytic activity against antibiotic-resistant *A. baumannii* strains.

Methods: Five parameters were screened using a 12-run PB design: the concentrations of glucose, glycerol, $MgSO_4.7H_2O$, lactose, as well as lactose addition time. Recombinant endolysin was extracted from the *E. coli* cells obtained in each run, and its activity was determined using a turbidity reduction assay against an antibiotic-resistant *A. baumannii* strain.

Results: Analysis of Variance (ANOVA) revealed that glucose, glycerol, and lactose significantly influenced recombinant endolysin production and lytic activity ($P<0.05$), whereas $MgSO_4.7H_2O$ and lactose addition time showed no significant effects. The results reflected screening-level functional activity rather than quantitative protein expression. The Plackett–Burman screening identified glucose, glycerol, and lactose as significant factors influencing endolysin activity. A positive linear correlation was observed between increasing glycerol and lactose concentrations and higher endolysin activity, whereas the effect of glucose was observed within a relatively narrow concentration range. The condition corresponding to the highest activity within the tested PB matrix was observed at low glucose (0.0247% w/v), high glycerol (5.92% w/v), and high lactose (4.880% w/v).

Conclusion: These findings highlight the key factors influencing endolysin production and provide a basis for subsequent detailed optimization studies.

Keywords: Endolysin, *Acinetobacter baumannii*, Antibiotic resistance, Autoinduction Medium, Plackett-Burman design, Screening

Please cite this article as follows: Rafighi D, Azin M, Akhavan Sepahi A, Alimadadi N. Screening of key auto-induction medium components affecting recombinant endolysin production against antibiotic-resistant acinetobacter baumannii using a plackett–burman design. Avicenna J Clin Microbiol Infect 2026;13(3): x-x. doi:10.34172/ajcmi.3777

Introduction

Antibiotic resistance is now a worldwide health emergency, driven in part by the inappropriate and excessive use of antibiotics in humans (1, 2). Such misuse has contributed to the production of antibiotic-resistant pathogens, making infectious diseases unrestrained (3). The crisis highlights the need for effective antibiotic stewardship, the development of novel therapeutic approaches, and continued research aimed at combating microbial resistance. In vitro antimicrobial susceptibility testing is critical for determining resistance levels, particularly with the rising incidence of multidrug-resistant (MDR) microorganisms and the limitations of current therapeutic strategies (4).

Acinetobacter baumannii is a Gram-negative, aerobic, non-fermenting bacterium that is widely distributed in soil, water, and air. The bacterium colonizes various host sites, including the conjunctiva, oral mucosa, skin, and the respiratory, gastrointestinal, and urogenital tracts (5). *A. baumannii* has emerged as an important virulent pathogen due to its strong adherence, high colonization rates, desiccation tolerance, and resistance

to commonly used disinfectants and ultraviolet light. These features contribute to its role as an etiologic agent of nosocomial infections, particularly among critically ill immunocompromised patients, manifesting as wound infections, central nervous system (CNS) complications, abdominal and urinary tract infections, and bacteremia (6). Consequently, the World Health Organization (WHO) has categorized *A. baumannii* as a "critical priority" pathogen because of its persistence and emergent resistance patterns (7). Its clinical importance has increased over the past fifteen years owing to the presence of multiple resistance determinants. Consequently, certain isolates are resistant to all antimicrobial classes currently available for clinical use, thereby necessitating an immediate international public-health response (8).

Due to the growing challenge of antibiotic resistance, research has focused on the discovery of new antimicrobial agents as effective alternatives to traditional antibacterial drugs (9). One such group is endolysins, which are proteins produced during the bacteriophage lytic cycle. These proteins facilitate the release of virions through the enzymatic degradation of the peptidoglycan layer of bacterial cell walls (10). Unlike conventional antibiotics, endolysins exhibit high specificity and act against pathogenic bacteria without harming the beneficial commensal microbiota (11). They induce instant bacterial lysis, and the development of bacterial resistance to their activity appears less likely. Endolysins have also been effectively utilized in combination with other antimicrobials, showing synergistic activity against recalcitrant infections (12). They possess considerable potential for the treatment of chronic and biofilm infections due to their intrinsic ability to penetrate the biofilm matrix and lyse bacterial cell walls (10). Their distinctive bacteriolytic specificity and activity make endolysins promising therapeutic agents against drug-resistant bacterial infections (13). Therefore, recombinant endolysins have been extensively explored as antimicrobial agents against drug-resistant pathogens (14).

Following the discovery of genetic engineering tools in the 1970s, biology was transformed, and heterologous protein expression became a routine approach in biotechnology. Among the available prokaryotic and eukaryotic host-expression systems, the *Escherichia coli* expression system remains the most widely employed system for recombinant protein production (15). Laboratory- scale production of endolysins is typically accomplished using *E. coli* as the expression host. The target gene for endolysin is cloned into an appropriate expression vector and introduced into *E. coli*, which effectively expresses the gene to produce high levels of endolysin. Recombinant endolysins produced in *E. coli* are effective against drug-resistant pathogens and have desirable therapeutic potential (16). The major advantage of recombinant endolysins is their genetic manipulability, which allows their stability and antibacterial activity to be enhanced. However, challenges related to dose adjustment and large-scale production persist (11).

Although *E. coli* expression systems have several benefits, the production of recombinant endolysins at therapeutic doses remains challenging. Expression is typically chemically induced, for example, through the addition of isopropyl-β-D-thiogalactoside (IPTG) or lactose, and these processes can be time-consuming and labor-intensive (9). In controlled expression systems, supplying glucose at very low concentrations is a well-established strategy for preventing metabolic overflow and acetate accumulation. According to Shiloach and Fass (17), even moderate glucose concentrations can saturate central metabolism and inhibit growth in *E. coli;* therefore, minimal glucose concentrations are commonly used when stable expression and reduced metabolic stress are required. Expression must also be tightly controlled to prevent inclusion-body formation and achieve optimal protein solubility, thereby improving the final yield and biological activity (9).

Another system allows the production of recombinant protein under *lac* or T7 promoters in the absence of exogenous lactose or IPTG induction. Basal expression in such systems can yield high-level target protein without the need for exogenous inducers. Autoinduction, as described by Studier (18), is one approach that enables automated protein production without the need to monitor bacterial growth phases or control inducer timing (19). Glycerol is often preferred to glucose as the primary carbon source because it does not induce overflow metabolism and supports stable high-density growth, as demonstrated by Shiloach and Fass (17). Autoinduction provides a simple and effective approach for recombinant protein production and has been successfully applied to the production of recombinant endolysins at both laboratory and large-scale biopharmaceutical levels (19).

Autoinduction in culture media employs diauxic growth mechanisms to achieve optimal protein production. Glucose is preferentially utilized by bacterial cells to support cell mass accumulation. Upon glucose depletion, the cells subsequently utilize lactose as an alternative carbon source. This metabolic shift naturally induces target-gene expression and recombinant protein production, including the production of endolysins (20). An optimized formulation of autoinducing medium was initially recommended by Studier (18). Subsequently, Li et al developed an enhanced medium incorporating ammonium and phosphate salts, ferric citrate, citric acid, trace elements, and multiple carbon sources, including glucose, lactose, and glycerol (21).

Although endolysins possess significant antibacterial properties and autoinducing media have demonstrated benefits for recombinant protein production, limited research has focused on optimizing endolysin production against drug-resistant *A. baumannii*. This knowledge gap necessitates further investigation into the optimization of autoinducing media.

This research aimed to screen key autoinduction-medium components affecting recombinant endolysin production for potential medical applications against antibiotic-resistant *A. baumannii* strains. Because this study was designed as an initial screening investigation, functional activity, measured using the turbidity reduction

assay (TRA), was selected as the primary response variable rather than direct protein quantification. Environmental factors influencing the antibacterial activity of recombinant endolysins were examined. This research will provide a foundation for subsequent optimization protocols and help fight against antibiotic-resistant infections.

Material and Methods

Plackett–Burman Design

To screen the factors affecting recombinant endolysin production against antibiotic-resistant *A. baumannii*, a Plackett–Burman (PB) screening design was used. Five important parameters were investigated: glucose, glycerol, lactose, magnesium sulphate heptahydrate ($MgSO_4 \cdot 7H_2O$), and lactose addition time. These factors were selected based on their potential effects on enzyme expression under an autoinduction system. Twelve experimental conditions were generated in 500-mL Erlenmeyer flasks containing culture medium (Table 1). Enzyme activity was measured using the TRA at 4, 8, 12, and 16 hours after inoculation. The PB design was used to screen for significant factors using fewer experiments. Although it estimates major effects of the factors rather than their interactions, it is well suited for the first optimization studies. The experimental design was carried out using Minitab 22 software. Five factors were chosen empirically based on a literature review, including ZYM5052 medium constituents and conditions for optimal enzyme expression under the T7 promoter in autoinduction systems (18).

Five important parameters were selected to examine their influence on endolysin production in *E. coli* BL21(DE3), with their low and high levels established using Minitab software:

1. Glucose: 0.0247% w/v (low) and 0.2470% w/v (high), used as a regulatory metabolite and transient repressor.
2. Lactose: 0.488% w/v (low) and 4.880% w/v (high), used to regulate T7 promoter induction.
3. Glycerol: 1.48% w/v (low) and 5.92% w/v (high), serving as the principal carbon source for biomass growth.
4. $MgSO_4.7H_2O$: 0.5 mM (low) and 2 mM (high), serving as a magnesium source for enzymatic processes.
5. Lactose addition time: 4 hours (low) and 8 hours (high) after the initiation of bacterial growth.

The glucose concentration was intentionally maintained at extremely low levels to prevent overflow metabolism and acetate accumulation, consistent with recommendations of Shiloach and Fass (17). The PB design was used solely as a screening tool to determine the direction and significance of factor effects rather than to identify the true optimal concentrations. This design enabled efficient evaluation of factor significance with a minimal number of experimental runs. The PB results were subsequently used to select significant variables for further optimization using response surface methodology (RSM).

In this study, the glucose concentration was intentionally maintained at very low levels compared to those used in conventional autoinduction media. The rationale behind this choice was that glucose in autoinduction systems primarily functions as a regulatory metabolite that controls the timing of lactose induction rather than as the main carbon source. At high concentrations, glucose represses the *lac* operon through catabolite repression, thereby delaying the induction of recombinant protein expression. Conversely, a minimal glucose supply is rapidly depleted during the early exponential-growth phase, enabling an immediate metabolic shift toward glycerol and lactose utilization and triggering the autoinduction phase. Thus, in the present study, glucose functioned as a transient repressor that synchronized the metabolic transition and supported endolysin expression. Glycerol served as the main carbon source for biomass formation, whereas lactose functioned as the natural inducer under T7 promoter regulation.

Pre-culture Preparation

E. coli BL21 (DE3) was inoculated in Terrific Broth medium supplemented with 50 µg/mL kanamycin and incubated at 37°C with agitation at 180 rpm. Cultivation continued until

Table 1. Experimental Conditions Offered by Minitab Software

Flask Number	Base Medium Volume (mL)	$MgSO_4.7H_2O$ (mM)	Glucose (%w/v)	Glycerol (%w/v)	Lactose (%w/v)	Lactose Addition Time (hours)
1	36.44	2.0	0.0247	1.48	0.488	8
2	26.98	0.5	0.2470	1.48	4.880	8
3	26.92	2.0	0.2470	1.48	4.880	8
4	19.3	0.5	0.0247	5.92	4.880	4
5	26.8	0.5	0.0247	1.48	4.880	4
6	28	2.0	0.0247	5.92	0.488	8
7	19.92	2.0	0.2470	5.92	4.880	4
8	28.48	0.5	0.2470	5.92	0.488	8
9	36.42	0.5	0.0247	1.48	0.488	4
10	36.42	2.0	0.2470	1.48	0.488	4
11	28.48	0.5	0.2470	5.92	0.488	4
12	19.92	0.5	0.0247	5.92	4.880	8

Note. $MgSO_4 \cdot 7H_2O$: Magnesium sulfate heptahydrate; mM: Millimolar; h: Hours.

the optical density at 600 nm (OD_{600}) reached approximately 0.6, which is the exponential growth phase with maximum protein expression. This phase supports a high metabolic rate and growth, which are optimal for recombinant protein expression under T7 promoter control. Terrific Broth medium, providing a rich source of nitrogen and carbon, facilitates higher cell density compared to Luria-Bertani medium. Its formulation, comprising tryptone, yeast extract, glycerol, and phosphate buffer, is designed to enhance cell growth and achieve high optical density, making it ideal for the large-scale production of proteins and frequent expression of the gene.

Culture Conditions

Following *E. coli* BL21(DE3) pre-culture preparation, sterile 500 mL Erlenmeyer flasks containing 40 mL of culture medium were used to ensure adequate aeration during growth and protein expression. The ZYM5052 medium consisted of NZ-Amine (peptones and nitrogen), yeast extract (nucleotides, vitamins, and growth factors), Na_2HPO_4 and KH_2PO_4 (pH control), NH_4Cl (inorganic nitrogen source), Na_2SO_4 (sulfate ions), and trace element solution (Fe^{2+}, Mn^{2+}, Zn^{2+}, Co^{2+}, Cu^{2+}). Kanamycin was added for continuous plasmid selection from a 50 mg/mL stock solution at a final concentration of 50 µg/mL (40 µL/40 mL medium). Glucose, glycerol, lactose, $MgSO_4.7H_2O$, and trace elements were prepared separately as stock solutions and sterilized by filtration through 0.22-µm membrane filters to avoid compound degradation. They were then added to the basal medium under aseptic conditions.

After preparing the culture media according to the component amounts generated by Minitab software, 40 mL of each autoinduction medium was dispensed into each Erlenmeyer flask. Each flask was inoculated with 1% v/v (400 µL) of the prepared *E. coli* BL21(DE3) pre-culture under sterile conditions. The flasks were incubated at 37°C for 16 hours with agitation at 250 rpm. To evaluate the effects of culture conditions on endolysin production and growth indicators, samples were collected at 4, 8, 12, and 16 hours post-inoculation for wet-cell biomass measurement, residual glucose determination, and lytic activity assessment by TRA. All biomass determinations were carried out in three independent replicates to obtain reproducible and consistent results. This parameter serves as an indirect indicator of the cells' metabolic activity and protein-synthesis capacity among flasks, as higher intracellular water content is characteristically associated with active metabolism and rapid protein synthesis.

A full time-course assay was performed for all 12 PB conditions. A standardized pre-culture grown to OD600 ≈ 0.6 was used to inoculate each flask, and samples were collected at 4, 8, 12, and 16 hours post-inoculation. TRA measurements were carried out independently for every time point and every flask. In all conditions, the highest lytic activity was reproducibly observed at 12 hours, which was therefore selected as the measurement time point for the PB comparisons.

Biomass Determination (Wet and Dry Cell Weight)

To quantify the biomass produced under each PB condition, 15 mL of the culture was collected from each flask at the designated sampling time. All biomass measurements were performed in three independent biological replicates to ensure reproducibility.

Each 15-mL sample was transferred into a pre-weighed tube and centrifuged at 8000 rpm for 10 minutes at 4°C. The supernatant was discarded, and the tube containing the cell pellet was immediately weighed to obtain the wet weight (WW). The tube was then placed in a drying oven at 90°C until a constant weight was achieved, which typically required 5-6 hours. After drying, the tube was cooled to room temperature in a desiccator and weighed again to obtain the dry weight (DW). The difference between the two values was calculated using the following expression.

$$\Delta(WW–DW) = WW - DW$$

This parameter represents the total moisture-associated portion of the biomass present in a 15 mL culture sample. It was used solely as a qualitative indicator for comparing relative biomass accumulation across the different PB experimental conditions. All biomass-related data reported in the Results section correspond to 15-mL culture volumes.

Residual Glucose Determination

Residual glucose levels were measured using the 3,5-dinitrosalicylic acid (DNS) method (22). Optical absorbance was read at 540 nm using a spectrophotometer. Glucose concentrations were calculated from a standard curve constructed with glucose solution (0.25, 0.5, 0.75, and 1 mg/mL). Samples were diluted within the linear range of the assay.

Turbidity Reduction Assay

For TRA analysis (23, 24), cells harvested at 4, 8, 12, and 16 hours were centrifuged at 8000 rpm for 10 minutes at 4°C. The cell pellets were washed twice with phosphate buffer (50 mM, pH 7.4) and stored frozen for further processing.

Antibiotic-resistant *A. baumannii* was cultivated in Tryptic Soy Broth (TSB) at 37°C with shaking at 180 rpm until OD_{600} was 0.6. Once exponential growth was achieved, the bacterial suspension was centrifuged at 8000 rpm for 10 minutes. The pellet was washed and resuspended in phosphate-buffered saline (PBS) containing 1 mM EDTA.

The *E. coli* BL21(DE3) pellets were resuspended in PBS buffer (pH 7.4) supplemented with 10% glycerol, 0.1% mercaptoethanol, and 0.5 mg/mL lysozyme. After a 2-hour incubation on ice with gentle agitation (100 rpm), the cells were sonicated using an ultrasonic homogenizer for 5 minutes (30 seconds on/off cycles) at 70% amplitude on an ice bath. The cell lysate was centrifuged at 12000 rpm for 15 minutes at 4°C. The supernatant containing the soluble endolysin was collected and used for the TRA (23, 24).

TRA was performed at 12 hours post-inoculation, which had been established as the time of peak endolysin activity during the initial time-course experiments conducted at 4, 8, 12, and 16 hours. Lysozyme (0.5 mg/mL; Sigma-Aldrich) was used as a positive control, while PBS (pH

7.4) was used as a negative control. Lysozyme was selected as a standardized, reproducible, and commercially available benchmark for assay validation in the presence of EDTA. Although lysozyme primarily targets Gram-positive bacteria, numerous studies have demonstrated that EDTA-treated Gram-negative cells, including *A. baumannii*, become permeable to lysozyme, making it a widely accepted reference control to verify the performance and dynamic range of turbidity reduction assays. The positive control lowered OD_{600} by approximately 70–80% after 1 hour of incubation at 37°C, confirming the reproducibility of the assay. Each TRA was performed in triplicate by mixing 500 µL of the *A. baumannii* suspension with 500 µL of the enzyme solution. Turbidity reduction was expressed as the percentage decrease in OD_{600} relative to the negative control, allowing comparison among replicates.

The lysozyme control sustained assay conditions at full capacity and ensured that the observed decreases in turbidity were attributable to recombinant endolysin activity rather than other factors. All samples were treated identically under the same conditions (37°C, 250 rpm, 60 min). Replicate consistency of lysozyme-induced lysis ensured assay precision and sensitivity for comparison.

Following preparation of the *A. baumannii* cell suspension and endolysin preparation, 500 µL of *A. baumannii* suspension in PBS+EDTA was mixed with 500 µL of endolysin solution. The samples were incubated at 37°C for 1 hour with shaking at 250 rpm. The negative control contained PBS+EDTA without enzyme, whereas the positive control contained lysozyme (0.5 mg/mL). OD_{600} was measured before and after incubation. The positive control confirmed that lytic enzymes could considerably reduce turbidity and serve as a reference for evaluating recombinant endolysin activity. Comparison of turbidity reduction relative to the negative control revealed the lytic activity of the enzyme preparations and enabled comparison of experimental outcomes among different culture conditions. This assay was used as the sole response parameter in accordance with the screening nature of the PB design.

In this study, the functional assay (TRA) was used as the primary indicator of active recombinant endolysin production. Protein quantification and electrophoretic characterization, including Bradford protein assay and SDS-PAGE, were not performed at this screening stage and are planned for future confirmatory experiments.

Validation Experiments

For validation of the condition identified as Flask 4, three independent biological replicates were performed. Each replicate was initiated from a freshly streaked single colony, followed by the preparation of a fresh preculture grown to an OD600 ≈ 0.6. A new 40-mL autoinduction culture was inoculated for each validation run, and all subsequent steps, including incubation, induction, harvesting, cell lysis, and TRA measurement, were carried out independently. No samples, lysates, or cultures from the original PB experiment were reused.

Results

Statistical analysis of the PB experimental design data using Minitab 22 revealed the effects of individual factors on recombinant endolysin-associated lytic activity. The concentrations reported represent the highest TRA values observed among the PB runs, rather than optimized protein expression levels. The graphical tools like Normal Plot, Half Normal Plot, and Pareto Chart of Standardized Effects (Figure 1) isolated the factors that had a profound effect on endolysin yield and activity.

Preliminary time-course analysis across all 12 PB conditions showed that lytic activity consistently peaked at 12 hours; therefore, all reported TRA values corresponded to this experimentally validated time point.

Despite the low glucose content, cell growth proceeded normally, which agrees with documented observations that minimal glucose levels can support balanced metabolism when glycerol is present as the main carbon source.

The Pareto chart (Figure 1) is a robust technique for ranking factors according to the magnitude of their standardized effects and for displaying a reference line for statistical significance. Conventionally, this significance threshold is set at the 95% confidence level corresponding to a $P < 0.05$ and is used to differentiate statistically significant from non-significant factors.

Statistical modeling identified glucose ($P = 0.003$), glycerol ($P = 0.002$), and lactose ($P = 0.002$) as significant factors influencing recombinant endolysin-associated lytic activity ($P < 0.05$). In contrast, $MgSO_4.7H_2O$ ($P = 0.142$) and lactose-addition timing ($P = 0.266$) showed no statistically significant effects. The overall model ($P = 0.002$) was an effective predictor of the experimental response.

Analysis of Variance (ANOVA) (Table 2) verified the statistical significance of the PB model (Table 2). The regression model was significant ($P = 0.002$). Glucose, glycerol, and lactose indicated statistically significant effects, with low *P*-values (0.003 and 0.002, respectively) and high *F*-values (24.31, 29.09, and 29.09, respectively), showing that their effects were greater than the unexplained variance. In contrast, $MgSO_4.7H_2O$ ($P = 0.142$) and lactose-addition timing ($P = 0.266$) were not statistically significant ($P > 0.05$). These ANOVA results supported the inferences

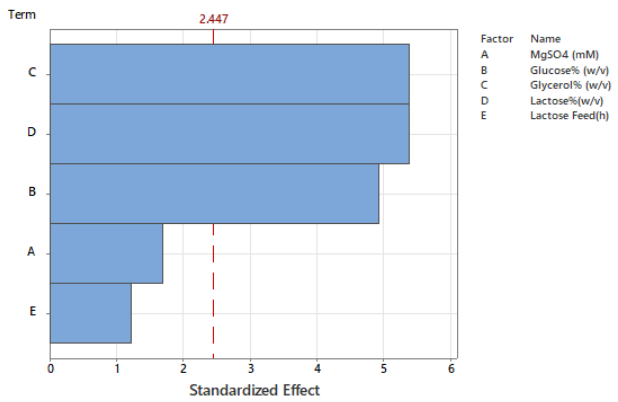

Figure 1. Pareto Chart of Standardized Effects

obtained from the Pareto chart and other graphical analyses.

The statistical significance of glucose, glycerol, and lactose ($P<0.05$) indicates consistent experimental effects; s; however, it does not establish absolute biological causation. To verify the reproducibility of the screening outcome, the condition corresponding to Flask 4 was re-evaluated using three fully independent biological replicates. Each replicate was performed using a newly prepared culture started from a fresh single colony. The mean lytic activity obtained from these independent validation runs was 73.2 ± 3.1%, demonstrating that the high TRA response associated with Flask 4 was consistently reproduced when the complete workflow was repeated from the beginning. These data confirm the biological reproducibility of the observed effect and indicate that it was not attributable to repeated measurements of a single preparation.

$MgSO_4.7H_2O$ showed no significant effect within the PB screening range ($P=0.142$). As is typical for PB screening designs, non-significant factors were interpreted conservatively. Similarly, lactose-addition time ($P=0.266$) showed no statistically significant effect. Therefore, these factors were not prioritized for further investigation during this screening stage, allowing subsequent studies to focus on the leading factors.

Biomass Assessment Across Plackett–Burman Conditions

The wet and dry biomass values obtained from 15-mL culture varied across the 12 PB conditions. Table 3 summarizes the calculated Δ(WW–DW) values for each flask. These values were used to compare relative biomass accumulation associated with each medium composition. All measurements represent the mean of three independent biological replicates, and the results were consistent across replicates.

Among all conditions, Flask 7 exhibited the highest biomass level, with a Δ(WW–DW) value of approximately 2.00 g per 15 mL culture, while Flask 9 showed the lowest value. This trend was consistent with the visual density of the cultures and indicated that the biomass yield varied substantially depending on the carbon-source composition.

Because the PB design was intended for qualitative factor screening, the Δ(WW–DW) values were used only to compare biomass trends among experimental conditions rather than to derive metabolic interpretations.

Main-effects and interaction plots were examined following ANOVA results. The main-effects plots (Figure 2) validated the positive effects of glucose, glycerol, and lactose on endolysin-associated lytic activity at higher concentrations. The interaction plots (Figure 3) showed synergistic relationships among these potent variables. In particular, the non-parallel glucose-glycerol interaction lines suggested that the effect of glucose may depend on glycerol concentration. Similarly, the glucose-lactose and glycerol-lactose interactions suggested possible combined effects of these factor pairs on the response. These graphical findings corroborated the ANOVA findings by supporting the individual and interdependent significance of the three factors.

Glucose, glycerol, and lactose were significant factors associated with recombinant endolysin-associated lytic activity. Their positions above the significance line in the Pareto chart further supported their importance in maximizing endolysin activity. In contrast, $MgSO_4{\cdot}7H_2O$ and lactose-addition time had no significant impact on the response. Both parameters were below the significance line in the Pareto chart, suggesting that the tested variations did not influence endolysin production or lytic efficiency. This finding is useful in simplifying large-scale processes.

Contour plots (Figures 4-6) represent the three-dimensional interactions among glucose, glycerol, and lactose, showing peak endolysin production regions. Response (%) was used to measure endolysin activity as the percentage reduction in bacterial turbidity. Higher values signify greater lytic activity in the hydrolysis of bacterial cell walls. The plots illustrate how the carbon sources (glucose, glycerol) and the inducer (lactose) regulate the production and activity, as well as their combined effects on final endolysin yield.

Higher concentrations of glycerol and lactose, along with

Table 2. ANOVA of the Significant Factors

Source	DF	Adj SS	Adj MS	*F*-value	*P*-value
Model	5	2990.86	598.17	15.89	0.002
Linear	5	2990.86	598.17	15.89	0.002
$MgSO_4.7H_2O$ (mM)	1	107.53	107.53	2.86	0.142
Glucose (%w/v)	1	914.82	914.82	24.31	0.003
Glycerol (%w/v)	1	1094.77	1094.77	29.09	0.002
Lactose (%w/v)	1	1094.77	1094.77	29.09	0.002
Lactose Feed Time (h)	1	56.49	56.49	1.50	0.266
Error	6	225.81	37.63		
Total	11	3216.67			

Note. ANOVA: Analysis of variance; DF: Degrees of freedom; SS: Sum of squares; MS: Mean square; $MgSO_4{\cdot}7H_2O$: Magnesium sulfate heptahydrate; mM, millimolar.

Table 3. Estimated Δ(WW–DW) Values for *E. coli* BL21) DE3) Under Different Plackett–Burman Conditions

Flask No.	Estimated Δ(WW–DW) for 15 mL (g)
7	2.00 g
8	1.85 g
4	1.70 g
12	1.60 g
6	1.50 g
11	1.40 g
2	1.30 g
3	1.20 g
10	1.10 g
5	1.00 g
1	0.90 g
9	0.80 g

Note. Δ(WW–DW): Difference between wet weight (WW) and dry weight (DW); *E. coli*: *Escherichia coli*.

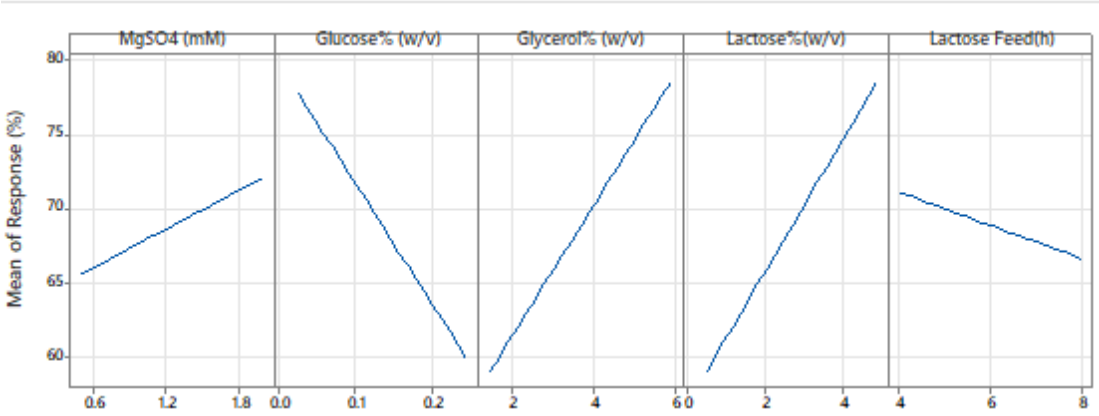

Figure 2. Main Effects Plots

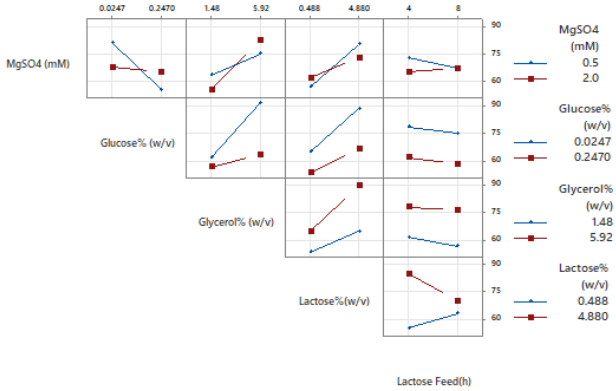

Figure 3. Interaction Plots

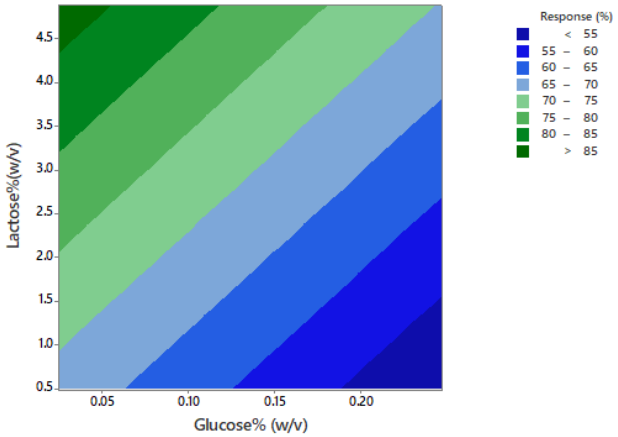

Figure 5. Contour Plot of Response (%) vs Glucose% (w/v), Lactose% (w/v)

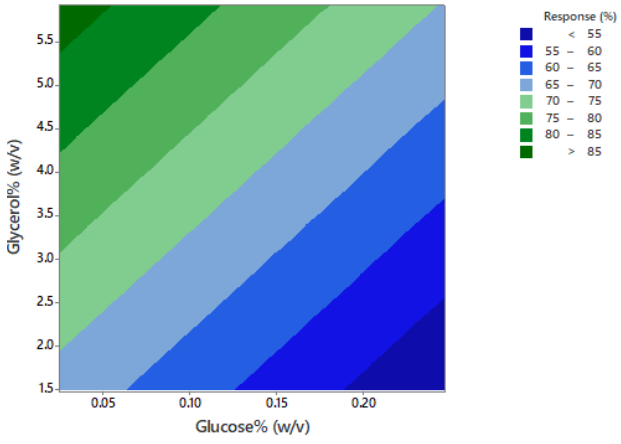

Figure 4. Contour Plot of Response (%) vs Glucose% (w/v), Glycerol% (w/v)

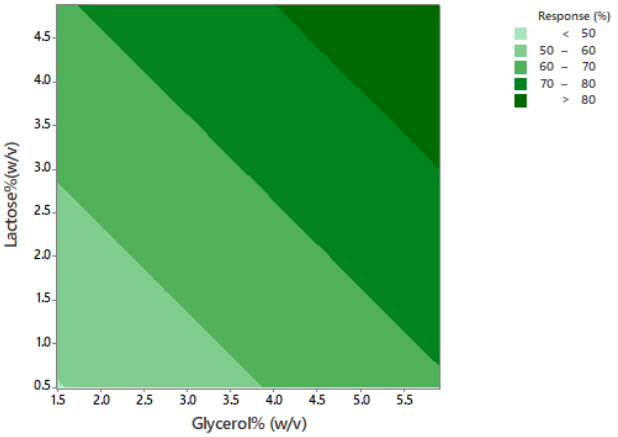

Figure 6. Contour Plot of Response (%) vs Glycerol% (w/v), Lactose% (w/v)

low glucose concentration, were associated with increased endolysin activity. Glucose is essential for initial cell growth and, upon its depletion, lactose induces autoinduction to achieve optimal endolysin production.

Conclusions drawn from the contour-plot analysis were consistent with the PB model in identifying the condition with the highest activity within the tested range. The highest-performing condition among the screening runs was observed at 0.0247 w/v glucose, 5.92 w/v glycerol, and 4.880 w/v lactose. This confirms the ability of the PB model to identify significant factors; however, no statistical optimum is claimed because PB is a screening design.

To evaluate the validity of the PB statistical model used for data analysis and response prediction in this study, plots concerning residuals were carefully examined. Residuals represent the differences between measured enzyme-activity values obtained from the experimental runs and the corresponding values predicted by the statistical model. Examination of these discrepancies is important for determining the adequacy, accuracy, and precision of the model.

The normal probability plot of residuals (Figure 7)

showed an approximately straight-line pattern. It suggests that the residuals were reasonably consistent with a normal distribution, indicating the absence of major systematic bias and supporting the validity of the statistical model.

Furthermore, the residuals-versus-fits plot (Figure 8), a secondary diagnostic plot, showed that the residuals were randomly scattered about the zero line without a visible pattern. This random scatter suggests that the variance of errors was uniform across the complete range of results. These findings indicate that the model adequately explained the variations observed in the data nd produced reliable predictions within the investigated ranges.

These findings support the robustness and reliability of the PB model for determining significant factors and correctly predicting responses for recombinant endolysin activity. The statistical validation provides a sound basis for the inferences drawn from this screening study and for subsequent optimization of endolysin production.

The performance of the positive and negative controls was carefully monitored in all TRA assays. The lysozyme positive control produced a mean OD_{600} reduction of 76 ± 3%, demonstrating the effectiveness of the assay conditions and serving as a benchmark for recombinant endolysin activity. Under the Flask 4 screening condition, recombinant endolysin achieved approximately 85% of the lytic efficiency observed for lysozyme, confirming its strong antibacterial effect against drug-resistant *A. baumannii*. All TRA experiments were performed in triplicate, with variation of less than ± 5% among replicates, indicating high reproducibility and statistical reliability of the obtained results.

Sampling for the TRA assay was performed consistently at 12 hours post-inoculation for all experimental runs, as this time corresponded to the peak enzyme activity observed in the preliminary assays. This approach ensured comparability among all culture conditions and minimized time-related variation in lytic activity.

Biomass analysis, including WW and DW, revealed distinct patterns among different experimental flasks. Flask 7 exhibited the highest biomass accumulation (wet and dry weight), while Flask 4 showed lower biomass accumulation but the highest lytic activity in the TRA. These results were consistent across three independent replicates, confirming their reliability.

Discussion

The present study employed a PB design to screen five key medium components in an autoinduction system for their influence on recombinant endolysin activity produced by *E. coli* BL21(DE3). Because PB is a first-level screening tool rather than an optimization design, the primary objective of this work was to identify the environmental factors with the strongest effects on endolysin activity rather than to determine precise optimal concentrations. Accordingly, the results should be interpreted within the methodological scope of the PB design.

The screening experiment identified glycerol, glucose, and lactose as the major contributors influencing recombinant endolysin activity within the tested ranges. These findings align with the established physiology of lac-based autoinduction systems, in which glycerol serves as a non-phosphotransferase system (non-PTS) carbon source that supports high biomass formation and protein expression; glucose functions transiently to maintain catabolite repression, and lactose promotes induction after glucose depletion. This finding aligns with the findings of Shiloach and Fass (17), who reported that glycerol can be an effective carbon source for recombinant *E. coli*, as it can reduce overflow metabolism and support protein productivity. The observation that these three variables were statistically significant is therefore consistent with known regulatory mechanisms governing T7 promoter–based expression systems.

As expected for PB methodology, the interpretation of factor effects is qualitative and directional. The significant effects observed for glycerol, glucose, and lactose indicate that these components play significant roles in shaping the metabolic environment required for active endolysin expression. Conversely, $MgSO_4 \cdot 7H_2O$ and lactose addition time did not exhibit statistically significant effects within the tested ranges. Because PB designs do not estimate interaction effects and have limited statistical power by design, factors with non-significant or borderline *P*-values, such as $MgSO_4 \cdot 7H_2O$, should be interpreted conservatively

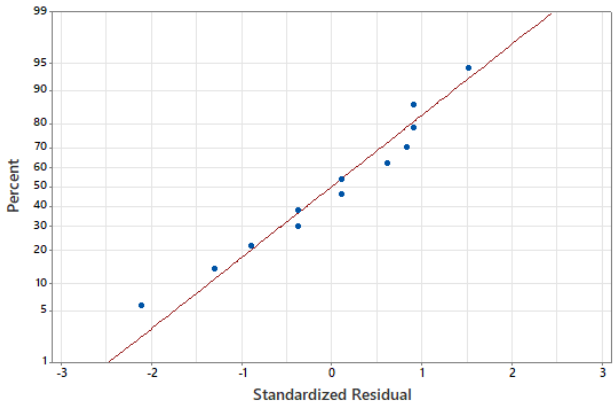

Figure 7. Normal Probability Plot of Residuals

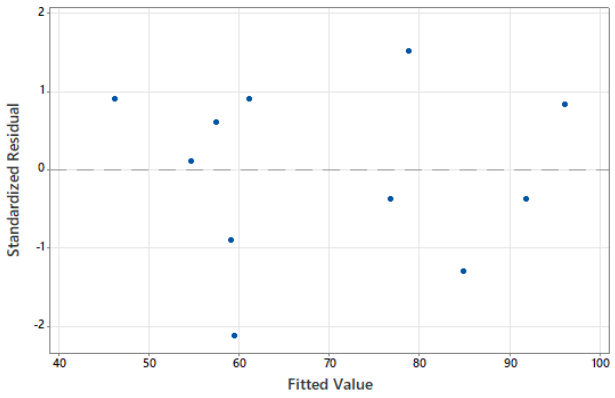

Figure 8. Residuals vs Fits Plot

during preliminary screening. This approach is consistent with the standard application of PB analysis in microbial bioprocess engineering.

An important observation was that biomass accumulation did not correlate directly with endolysin activity. For example, Flask 7 exhibited the highest biomass accumulation but did not produce the highest lytic activity, while Flask 4, despite lower biomass, demonstrated the strongest functional activity in the TRA assay. This dissociation between growth and enzyme activity is well recognized in recombinant protein expression systems, where high biomass can sometimes correspond to increased metabolic burden, folding stress, or diversion of cellular resources away from productive expression. Thus, the results highlight that the metabolic environment leading to high cell density is not necessarily the same environment that favors the production of biologically active endolysin.

The superior lytic activity observed in Flask 4 can be mechanistically explained by the coordinated effect of its specific glucose, glycerol, and lactose combination on central carbon metabolism, cellular energy status, and the dynamics of T7-driven protein expression. Although the PB design only identifies influential factors, the metabolic context underlying the enhanced production of functionally active recombinant endolysin under this condition can be reasonably explained based on established principles of *E. coli* physiology.

Low glucose levels in Flask 4 likely provided only a brief period of carbon catabolite repression (CCR). At trace concentrations, glucose is rapidly transported through the PTS, maintaining EIIA ^{Glc} predominantly in its dephosphorylated form and temporarily suppressing lactose uptake. This short repression window may prevent premature T7 RNA polymerase expression, which could otherwise impose substantial metabolic burden when induction occurred too early. Once glucose is depleted, EIIA ^{Glc} becomes phosphorylated, allowing lactose transport and allolactose formation to initiate T7-driven transcription. Because the glucose concentration was intentionally low, induction likely occurred at a moderate cell density, when the translational machinery remained active but was not yet stressed. This physiological state may favor the production of properly folded recombinant proteins rather than inclusion bodies.

Glycerol, present at relatively high concentration in Flask 4, served as the primary carbon and energy source without strongly inducing CCR because it is transported through a non-PTS pathway. Its metabolism supports a balanced NADH/NAD^+ ratio and provides high ATP generation without triggering overflow metabolism or acetate accumulation. This contrasts with higher-glucose conditions, where excessive glycolytic flux can lead to redox imbalance, acid stress, and impaired protein folding. Glycerol-driven metabolism therefore provides a stable energetic environment in which the synthesis, folding, and maturation of endolysin can proceed efficiently. The beneficial effect of glycerol is consistent with reports that glycerol supports slower but healthier growth, reduces misfolding, and increases the solubility of recombinant proteins expressed from the T7 system.

Lactose plays a central role in determining both the intensity and timing of induction. The moderate lactose concentration used in Flask 4 likely promoted controlled induction rather than a sharp transcriptional surge. Sudden high-level expression of T7 RNA polymerase can overwhelm the translation and chaperone systems, leading to misfolded or inactive protein. In Flask 4, however, lactose was present at a level sufficient to sustain induction while avoiding excessive metabolic burden. This moderated induction profile may have supported proper folding of the expressed endolysin, consistent with the high TRA activity observed under this condition.

The combined metabolic behavior of the three carbon sources in Flask 4 therefore appears to have created a highly favorable physiological state for recombinant protein production. Brief CCR mediated by low glucose may have prevented premature induction; glycerol provided a stable energy supply while minimizing overflow metabolism, and lactose provided a gradual and controlled induction phase. Together, these coordinated effects supported the production of soluble and active recombinant endolysin rather than merely increasing biomass or total protein content. This mechanistic framework explains why Flask 7, despite producing the highest biomass, did not yield the highest activity. High biomass conditions may be associated with redox imbalance or protein-folding stress, whereas Flask 4 achieved a more favorable balance among growth, energy metabolism, and induction dynamics for functional protein production.

To support the qualitative comparison of biomass across conditions, wet and dry cell weight measurements were performed using 15-mL culture samples. The calculated WW–DW differences served solely as auxiliary indicators of relative biomass accumulation and were not used to infer metabolic rates. This interpretation is consistent with the purpose of PB screening, which seeks only to identify influential variables rather than to construct physiological models. All biomass measurements were conducted using independent biological replicates to ensure reliability.

The use of a fixed 12-hour time point did not introduce bias because a complete time-course experiment, including 4, 8, 12, and 16 hours post-inoculation, was performed for every PB condition using the same inoculum source. In all 12 medium compositions, the maximum lytic activity was observed at 12 hours. Therefore, selecting this time point ensured that TRA measurements reflected the experimentally validated activity peak for each condition.

The choice of lysozyme as the positive control was intentional, as lysozyme combined with EDTA is a well-established benchmark for Gram-negative bacterial lysis assays. Although lysozyme is not specific to *A. baumannii*, it provides a stable, reproducible, commercially standardized enzyme that enables consistent validation of assay performance. In contrast, no universally accepted purified *A. baumannii*-specific endolysin is available as a standard control, and different endolysins vary substantially

in activity and stability. Therefore, lysozyme served as an appropriate functional reference for confirming assay reliability during the PB screening stage.

Finally, the condition corresponding to Flask 4 was reproduced in three fully independent biological experiments, each initiated from a freshly streaked colony and a freshly prepared pre-culture. The reproducibility of the lytic activity across these independent experiments confirms that the screening signal associated with this condition is biologically robust, even though PB methodology does not aim to define an optimized condition.

Overall, this study provides a systematic screening-based assessment of environmental factors influencing recombinant endolysin activity in an autoinduction system. The findings establish the relative importance of key carbon sources and identify variables that warrant further investigation in subsequent optimization studies, such as response surface methodology RSM or fed-batch bioprocess development. As a preliminary screening effort, the results offer a valuable foundation for the rational improvement of endolysin production against antibiotic-resistant *A. baumannii*.

These results highlight the potential of autoinduction systems for mass production of antimicrobial proteins. In the context of the antibiotic-resistance crisis, successful production of therapeutic compounds is paramount to fighting resistant infections and preserving public health.

Our findings are consistent with those of Kataoka and Takasu, who developed IPTG-free autoinduction systems that produced higher recombinant protein levels than standard procedures (25). Similarly, the autoinduction approach used in the present study generated recombinant endolysin with desired lytic activity.

Tahara et al investigated lactose and glucose as inducers in autoinduction systems and reported that adding these sugars to Terrific Broth medium achieved induction levels comparable to those of commercial autoinduction media, with recombinant protein production at milligram-per-liter levels (19). These findings are similar to our research, which screened glucose, glycerol, and lactose as key components affecting recombinant endolysin activity. Both studies support the importance of glucose and lactose in *lac* operon-based autoinduction systems for protein production in *E. coli*. However, whereas Tahara et al screened additives in rich media, the present study directly screened carbon-source levels in autoinduction medium for their influence on endolysin activity.

Yuan et al described phage vB_AbaP_D2 endolysin Abtn-4, which exhibited broad-spectrum antibacterial activity against drug-resistant *A. baumannii* and inhibited biofilm formation (26). The present study similarly focused on recombinant endolysin production for potential application against antibiotic-resistant *A. baumannii*. Together, these studies highlight the therapeutic potential of endolysins in addressing antibiotic-resistant bacterial infections.

De la Fuente-Kratzborn et al investigated whether lactose-mediated autoinduction could enhance the production of active [NiFe] hydrogenase in *E. coli* and successfully produced active hydrogenase in EnPresso B medium (27). The present study is consistent with this approach, as both investigations explored lactose-mediated autoinduction as a cost-effective alternative to IPTG induction. However, their study focused on producing a complex enzyme (hydrogenase) in a fed-batch culture, while our study screened the effects of glucose, glycerol, and lactose concentrations of the autoinducing medium on recombinant endolysin production.

Garcia Torres et al evaluated the antibacterial activity of the phage endolysin Ab_H-1.5 against drug-resistant *A. baumannii* and reported high bactericidal activity with complete loss of bacterial viability (28). The present study supports these findings, as the recombinant endolysin preparation showed lytic activity against drug-resistant *A. baumannii*. In particular, the condition represented by Flask 4 resulted in severe turbidity reduction, indicating high lytic activity. These experiments suggest the potential of endolysins as promising antibacterial agents against resistant strains.

Similarly, Soontarach et al compared the efficacy of the endolysin LysAB1245 with that of colistin against colistin-resistant *A. baumannii* and reported enhanced bactericidal activity (29). The present study concurs with those observations, as the recombinant endolysin successfully lysed resistant *A. baumannii*, as evidenced by the marked turbidity reduction observed for flask 4, indicating extensive lytic activity. Together, these studies highlight the promise of endolysins as potential therapeutic drugs to combat antibiotic-resistant bacterial infections.

Although ANOVA and residual analyses demonstrated statistically significant effects of the key factors, biological validation was essential to confirm the model's accuracy. The optimized condition was therefore evaluated using fully independent biological replicates initiated from fresh single colonies, ensuring that the observed effect reflected true biological robustness rather than technical repetition. These independent experiments verified that the predicted increase in endolysin activity was reproducible across biological experiments. Thus, the PB model effectively captured the experimental trends and supported the reproducible enhancement of endolysin production under real biological conditions.

Conclusion

This study identified key autoinduction medium components affecting recombinant endolysin activity in *E. coli* BL21(DE3) against drug-resistant *A. baumannii*. The PB screening revealed that glucose, glycerol, and lactose were the most influential factors within the tested range.

Biomass analysis also showed that the flask with the highest enzymatic activity (Flask 4) differed from the flask with the highest biomass (Flask 7), suggesting that maximizing cell mass does not necessarily lead to greater functional protein synthesis. Rather, metabolic equilibrium and regulated induction are required to generate correctly

folded and biologically active endolysin. The repeatability of the Flask 4 screening result was verified by independent biological replicates, supporting the reliability of the identified influential factors.

These findings provide a basis for future optimization studies and offer useful information for developing cost-effective, efficient, and IPTG-free autoinduction media for the large-scale preparation of antimicrobial endolysins against drug-resistant *A. baumannii*. Further analyses, including SDS–PAGE, Bradford protein quantification, and Western blotting, should be conducted in subsequent optimization phases, as further optimization lies outside the scope of this screening study. The optimized combination of low glucose and elevated glycerol is physiologically justified, as supported by metabolic studies, including Shiloach and Fass (17), which highlight the importance of minimizing glucose-associated stress and relying on non-PTS carbon sources to enhance recombinant protein expression.

Limitations of the Study

As this work represents the PB screening phase, direct protein quantification and molecular characterization were not included and should be addressed in future optimization studies. The P–B design was employed solely to identify significant factors affecting functional endolysin activity, not to determine true optimal concentrations. Therefore, the condition with the highest TRA activity within the tested range should not be interpreted as a statistically optimized formulation. Subsequent RSM experiments are required to refine the medium composition and achieve true optimization.

Acknowledgments

This manuscript is derived from the Ph. D. thesis of Darna Rafighi. The authors gratefully acknowledge the support of the Islamic Azad University, Science and Research Branch. They particularly thank Dr. Nahid Bakhtiari for her technical assistance and Eng. Sanaz Jafari and Eng. Houshang Moradi for their valuable assistance during the experimental work. The authors also thank all individuals who participated in this study in some manner.

Authors' Contribution

Conceptualization: Dorna Rafighi; Mehrdad Azin
Data Curation: Dorna Rafighi
Formal Analysis: Dorna Rafighi; Mehrdad Azin
Funding Acquisition: Mehrdad Azin
Investigation: Dorna Rafighi
Methodology: Dorna Rafighi; Mehrdad Azin
Project Administration: Mehrdad Azin
Resources: Mehrdad Azin
Software: Dorna Rafighi
Supervision: Mehrdad Azin
Validation: Dorna Rafighi; Mehrdad Azin
Visualization: Dorna Rafighi
Writing – Original Draft: Dorna Rafighi
Writing – Review & Editing: Mehrdad Azin; Abbas Akhavan Sepahi; Nayyereh Ali Madadi

Competing Interests

The authors disclose that they have no financial or conflicting interests.

Ethical Approval

Not applicable.

Funding

This manuscript received no financial support, grant funding, or sponsorship from any public, commercial, or not-for-profit organization.

References

1. Islam MA, Islam MR, Khan R, Amin MB, Rahman M, Hossain MI, et al. Prevalence, etiology and antibiotic resistance patterns of community-acquired urinary tract infections in Dhaka, Bangladesh. PLoS One 2022;17(9): e0274423. doi:10.1371/journal.pone.0274423
2. Zhao XL, Chen ZG, Yang TC, Jiang M, Wang J, Cheng ZX, et al. Glutamine promotes antibiotic uptake to kill multidrug-resistant uropathogenic bacteria. Sci Transl Med 2021;13(625): eabj0716. doi:10.1126/scitranslmed.abj0716
3. Elshobary ME, Badawy NK, Ashraf Y, Zatioun AA, Masriya HH, Ammar MM, et al. Combating antibiotic resistance: mechanisms, multidrug-resistant pathogens, and novel therapeutic approaches: an updated review. Pharmaceuticals (Basel) 2025;18(3):402. doi:10.3390/ph18030402
4. Osei Sekyere J, Kerdsin A, Chopjitt P, Wendling CC. Editorial: community series - characterization of mobile genetic elements associated with acquired resistance mechanisms, volume II. Front Microbiol 2023;14:1230730. doi:10.3389/fmicb.2023.1230730
5. Carvalheira A, Silva J, Teixeira P. *Acinetobacter* spp. in food and drinking water - a review. Food Microbiol 2021;95:103675. doi:10.1016/j.fm.2020.103675
6. Shi J, Cheng J, Liu S, Zhu Y, Zhu M. *Acinetobacter baumannii*: an evolving and cunning opponent. Front Microbiol 2024;15:1332108. doi:10.3389/fmicb.2024.1332108
7. Elshamy AA, Kamal SK, Mahmoud MT, Elhasany AM, Shady AA, Mohamed SA, et al. Recent insights on phage therapy against multidrug-resistant *Acinetobacter baumannii*. AMB Express 2025;15(1):44. doi:10.1186/s13568-025-01837-1
8. Larsson DG, Flach CF. Antibiotic resistance in the environment. Nat Rev Microbiol 2022;20(5):257-69. doi:10.1038/s41579-021-00649-x
9. de Marco A. Recent advances in recombinant production of soluble proteins in *E. coli*. Microb Cell Fact 2025;24(1):21. doi:10.1186/s12934-025-02646-8
10. Khan FM, Rasheed F, Yang Y, Liu B, Zhang R. Endolysins: a new antimicrobial agent against antimicrobial resistance. Strategies and opportunities in overcoming the challenges of endolysins against gram-negative bacteria. Front Pharmacol 2024;15:1385261. doi:10.3389/fphar.2024.1385261
11. Murray E, Draper LA, Ross RP, Hill C. The advantages and challenges of using endolysins in a clinical setting. Viruses 2021;13(4):460. doi:10.3390/v13040680
12. Rahman MU, Wang W, Sun Q, Shah JA, Li C, Sun Y, et al. Endolysin, a promising solution against antimicrobial resistance. Antibiotics (Basel) 2021;10(11):1277. doi:10.3390/antibiotics10111277
13. Sabur A, Khan A, Borphukan B, Razzak A, Salimullah M, Khatun M. The unique capability of endolysin to tackle antibiotic resistance: cracking the barrier. J Xenobiot 2025;15(1):19. doi:10.3390/jox15010019
14. Abdelrahman F, Easwaran M, Daramola OI, Ragab S, Lynch S, Oduselu TJ, et al. Phage-encoded endolysins. Antibiotics (Basel) 2021;10(2):124. doi:10.3390/antibiotics10020124
15. Ojima-Kato T. Advances in recombinant protein production in microorganisms and functional peptide tags. Biosci Biotechnol Biochem 2024;89(1):1-10. doi:10.1093/bbb/zbae147
16. Choi YJ, Kim S, Bae S, Kim Y, Chang HH, Kim J. Antibacterial effects of recombinant endolysins in disinfecting medical equipment: a pilot study. Front Microbiol 2021;12:773640.

doi:10.3389/fmicb.2021.773640
17. Shiloach J, Fass R. Growing *E. coli* to high cell density--a historical perspective on method development. Biotechnol Adv 2005;23(5):345-57. doi:10.1016/j.biotechadv.2005.04.004
18. Studier FW. Protein production by auto-induction in high density shaking cultures. Protein Expr Purif 2005;41(1):207-34. doi:10.1016/j.pep.2005.01.016
19. Tahara N, Tachibana I, Takeo K, Yamashita S, Shimada A, Hashimoto M, et al. Boosting auto-induction of recombinant proteins in *Escherichia coli* with glucose and lactose additives. Protein Pept Lett 2021;28(10):1180-90. doi:10.2174/0929866528666210805120715
20. Rosano GL, Morales ES, Ceccarelli EA. New tools for recombinant protein production in *Escherichia coli*: A 5-year update. Protein Sci 2019;28(8):1412-22. doi:10.1002/pro.3668
21. Li Z, Kessler W, van den Heuvel J, Rinas U. Simple defined autoinduction medium for high-level recombinant protein production using T7-based *Escherichia coli* expression systems. Appl Microbiol Biotechnol 2011;91(4):1203-13. doi:10.1007/s00253-011-3407-z
22. Gusakov AV, Kondratyeva EG, Sinitsyn AP. Comparison of two methods for assaying reducing sugars in the determination of carbohydrase activities. Int J Anal Chem 2011;2011:283658. doi:10.1155/2011/283658
23. Dorawa S, Biniek-Antosiak K, Bejger M, Kaczorowska AK, Ciuchcinski K, Godlewska A, et al. Crystal structure, enzymatic and thermodynamic properties of the *Thermus thermophilus* phage Tt72 lytic endopeptidase with unique structural signatures of thermal adaptation. J Struct Biol 2025;217(3):108230. doi:10.1016/j.jsb.2025.108230
24. Plotka M, Kaczorowska AK, Morzywolek A, Makowska J, Kozlowski LP, Thorisdottir A, et al. Biochemical characterization and validation of a catalytic site of a highly thermostable Ts2631 endolysin from the *Thermus scotoductus* phage vB_Tsc2631. PLoS One 2015;10(9): e0137374. doi:10.1371/journal.pone.0137374
25. Kataoka K, Takasu A. IPTG-independent autoinduction of extracellular matrix proteins using recombinant *E. coli* as the expression host. Polym J 2021;53(2):385-91. doi:10.1038/s41428-020-00411-9
26. Yuan Y, Li X, Wang L, Li G, Cong C, Li R, et al. The endolysin of the *Acinetobacter baumannii* phage vB_AbaP_D2 shows broad antibacterial activity. Microb Biotechnol 2021;14(2):403-18. doi:10.1111/1751-7915.13594
27. de la Fuente-Kratzborn F, Fan Q, Neubauer P, Gimpel M. Application of lactose based autoinduction for heterologous production of an active [NiFe] hydrogenase in *E. coli*. Biotechnol Lett 2025;47(3):47. doi:10.1007/s10529-025-03594-4
28. Garcia Torres S, Henrich D, Verboket RD, Marzi I, Hahne G, Kempf VA, et al. Bactericidal effect of a novel phage endolysin targeting multi-drug-resistant *Acinetobacter baumannii*. Antibiotics 2025;14(2):162. doi:10.3390/antibiotics14020162
29. Soontarach R, Voravuthikunchai SP, Srimanote P, Chusri S. Efficacy of endolysin LysAB1245 combined with colistin as adjunctive therapy against colistin-resistant gram-negative bacteria. Antibiotics (Basel) 2025;14(6):538. doi:10.3390/antibiotics14060538